IEEE Access
Multidisciplinary ⋮ Rapid Review ⋮ Open Access Journal

Received 23 August 2022, accepted 29 September 2022, date of publication 17 October 2022, date of current version 21 October 2022.

Digital Object Identifier 10.1109/ACCESS.2022.3215266

RESEARCH ARTICLE

Geomagnetically Induced Current Analysis in Malaysian Power Transmission System

ZMNAKO MOHAMMED KHURSHID[1,2], NUR FADILAH AB AZIZ[1], (Member, IEEE), ZETI AKMA RHAZALI[1], AND MOHD ZAINAL ABIDIN AB KADIR[2], (Senior Member, IEEE)

[1]Institute of Power Engineering (IPE), Universiti Tenaga Nasional, Jalan IKRAM-UNITEN, Kajang, Selangor 43000, Malaysia
[2]Advanced Lightning, Power and Energy Research Centre (ALPER), Faculty of Engineering, Universiti Putra Malaysia, Serdang, Selangor 43400, Malaysia

Corresponding author: Nur Fadilah Ab Aziz (nfadilah@uniten.edu.my)

This work was supported in part by the Ministry of Higher Education (MOHE) of Malaysia under Grant FRGS/1/2018/TK04/UNITEN/02/6, and in part by Universiti Tenaga Nasional (UNITEN) through UNITEN Bold Grant.

ABSTRACT For many decades, Geomagnetically Induced Current (GIC) has posed a significant risk over the electrical power grid infrastructures worldwide. The phenomenon occurs due to geomagnetic disturbance (GMD) and related space weather events arising from solar activity. It represents a potential hazard to the secure and safe operation of electrical power grids by causing half-cycle saturation of grounded High Voltage (HV) power transformers, relay misoperation, and increased reactive power demand in the power systems. Previous studies have shown that the occurrence of intense GIC is not limited to high and mid-latitude regions, but powerful space weather events can also result in intense GIC in power systems located in lower geographic latitudes. This study aims to estimate GIC and its impacts on a Malaysian power grid. A network model of the grid was constructed by using the Power System Simulator for Engineering (PSS/E). This represents the first attempt to study GICs in south-eastern Asian power grids since a region is considered to have low GIC risk up to now. During the analysis, firstly, we exposed the entire power network which includes 500 kV, 275 kV, and 132 kV system voltages to different geoelectric field strengths in the 0–180° directions. The applied geoelectric fields were calculated based on benchmark value for 1 in 100 years of GMD events. Then we disconnected the 132 kV low voltage systems from the network model to investigate their influence on the calculated GICs. The results demonstrated that the most vulnerable substations to GMD events and experienced large GICs were those located in the middle of the Malaysian power network. The maximum GIC was recorded at substation 22 with the value of 44.58 A due to the peak electric field of 1.2 V/km at 100° field direction. Also, the results showed that the calculated GICs slightly increased when 132 kV systems were removed from the power network, especially at the substations directly connected to these systems.

INDEX TERMS Geomagnetically induced current, geomagnetic disturbances, space weather, energy, high voltage transformers, Malaysian power system.

I. INTRODUCTION

Geomagnetic disturbances (GMD) are considered one of the most hazardous space weather events related to solar activity. GMD drive the geomagnetically induced current (GIC) flow in man-made technology and trigger interests from many researchers globally. The most geoeffective solar disturbances are known as coronal mass ejections (CMEs). These CMEs are masses of magnetic clouds composed by particles that are emanated from the Sun from time to time during periods of intense solar activity. When CMEs strike the Earth, the magnetic field of the Earth which protects against the fast-moving plasma is compressed and causes fluctuation and enhancement of the existing electric currents in the ionosphere. The charged particles travel down in the polar regions through the magnetic field lines and cause auroras. Such interactions result in the rapid variation of the magnetic field on the Earth. This variation induces a

The associate editor coordinating the review of this manuscript and approving it for publication was Mehmet Alper Uslu.

geoelectric field on the Earth's surface and causes the GIC to flow through modern technological infrastructures [1], [2]. This GIC is a quasi-direct current (DC) (in the frequency range of millihertz or lower) that flows through grounded systems [3], [4], [5], such as communication systems [6], [7], oil and gas pipelines [8], [9] and power transmission networks with neutral grounded transformers [10], [11], [12], [13]. Transformers which are connected by transmission lines and designed to work via alternating current (AC) are the most affected components by a GIC, as illustrated in Fig. 1. The GIC flow in transformer windings generates a DC magnetic flux in the magnetic cores of the transformers and causes saturation half-cycle amplification due to the nonlinear response of the core material.

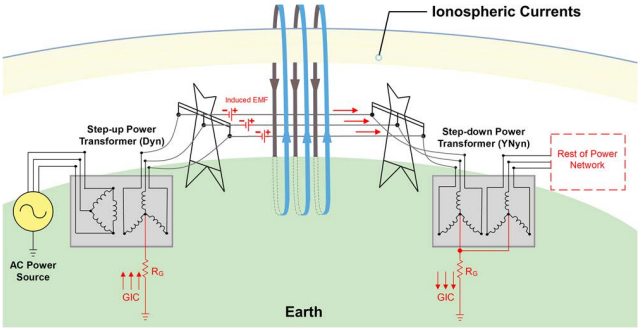

FIGURE 1. Description of GIC event in a power network.

This saturation generates harmonic currents and increases the reactive power consumptions of transformers leading to voltage instability of the system [14], [15], [16]. The harmonic currents can cause overheating of the windings and cores and vibration of the transformers, trigger improper relays, leading to unstable power system operations and may turn to long-term damage to the system's components or blackout. The GIC effects on power systems have been observed since the 1940s. The 1989 geomagnetic storm in North America is an instance of such catastrophic consequence due to the GIC effects that led to severe economic losses. The intensity of GIC strongly depends on the rate of time variation of the geomagnetic field, location of substations, ground resistivity, and system configuration. Grids with higher operational voltages imply smaller conductor resistance, making them more susceptible to carrying an intense GIC. Thus, the severity of a single GIC index could not be applied to all utilities. As a result of the aforementioned GMD events and effects, many power grid operators in various countries worldwide have begun to study and perform GIC measurements to assess the vulnerability of the power grid infrastructures. The presented incidents are clear examples of the impacts and severity of GMD on electrical power systems.

In addition, the review of earlier studies has shown that the GMD impacts are not limited to power grids in high and mid-latitudes but also extend to high voltage (HV) power grids at lower geographic latitudes [17]. In the previous work, we applied an extreme geomagnetic storm scenario on the modelled Malaysian power network and investigated the saturation effects of four HV power transformers and the effectiveness of the connected GIC mitigation systems to block GICs [18]. Therefore, this research aims to predict and investigate the effects of GMD on a Malaysian power grid, using geoelectric field magnitudes for low-latitude countries like Malaysia with consideration of the local geomagnetic latitude and earth conductivity structure with and without lower voltage system network. Note that the geographical location of Malaysia is close to the equatorial electrojet (EEJ) current. From the analysis, the GIC flow and reactive power losses are calculated for all transformers available in the system. A complete power system that considers all network parameters and variations are modelled using Power System Simulator for Engineering (PSS/E). The GIC is calculated in the Malaysian power transmission system due to the given geoelectric fields. The paper is organized as follows. In the second section, a Malaysian power network model is presented. In the third section, the applied geoelectric fields and methods used to estimate GIC in the Malaysian power grid are described. In the fourth section, the results and discussion are presented. Finally, the fifth section is the conclusion and perspectives of this paper.

II. MALAYSIAN POWER NETWORK

The power network in Peninsular Malaysia was modelled using the PSS/E software to investigate the GIC effects from different viewpoints. One of the advantages of PSS/E software is the availability of the GIC analysis tool as an integrated part of the power-flow analysis that can be performed in the program. The system model comprised of 138 buses located in 54 substations, interconnected through 71 power lines with different operating voltages such as 500 kV, 275 kV, and 132 kV transmission lines, as illustrated in Fig. 2. These line voltages are depicted in the figure as black, red and blue colours, respectively.

The system data are provided by the power utility company in Malaysia, Tenaga Nasional Berhad (TNB). GIC depends on the topology of the power system, which could be extremely vulnerable to certain geoelectric field directions and unaffected by other directions [19]. In addition, the higher operating voltages of the power system, implying low transmission line resistances, grid expansion, and low earth conductivity lead to the GIC intensity increase and its effects in most substations [14], [20]. The above-mentioned effects that caused the increase in GIC intensity were particular to other power grids and do not need to coincide in Malaysia.

In terms of rated voltages and winding types of available transformers in the model, they were divided into four types comprising 500 kV three winding auto, 275 kV three winding auto, 132 kV three winding, and 132 kV two winding transformers. The delta tertiary windings of transformers were connected to 3 kW loads through 415 V buses to avoid bus floating errors. However, all delta windings of transformers and loads were ignored during the GIC calculations since they do not provide the GIC flow paths. The data of transmission

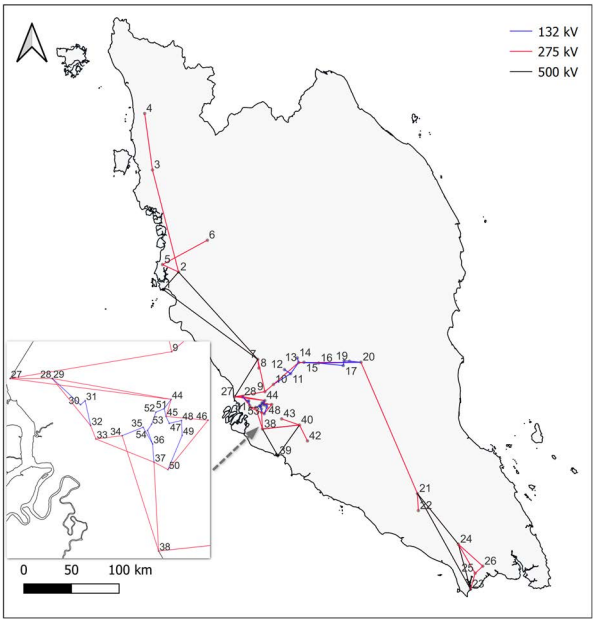

FIGURE 2. Power network in Peninsular Malaysia used for GIC analysis.

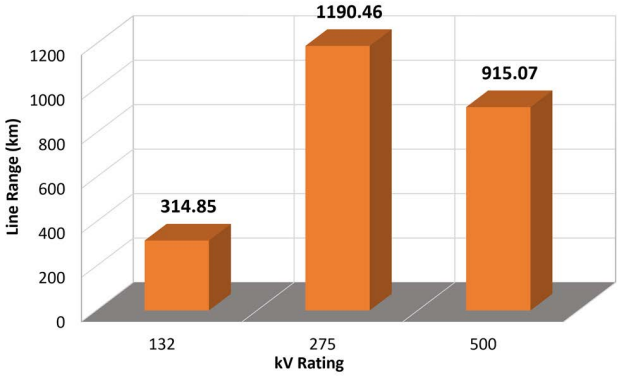

FIGURE 3. Transmission line length with the rated voltage used in the power network model.

lines and transformers are presented in Figs. 3 and 4, respectively.

This model is considered the first GIC estimation model of the Malaysian power network. The grounding resistance (GR) of all substations was set to 0.8 Ω. This value was within the recommended GR limit according to grid and distribution codes for Peninsular Malaysia [21], [22], [23]. The k-factors for all transformers have been set as 1. In large system studies, the default values for the k-factor often are used if actual data is unavailable [24]. Note that the k-factor value only affects the magnitude of the reactive power demands regarding the effective GIC.

A. GIC CALCULATION

A power grid vulnerability to GIC is made considering the benchmark geoelectric field. According to the North

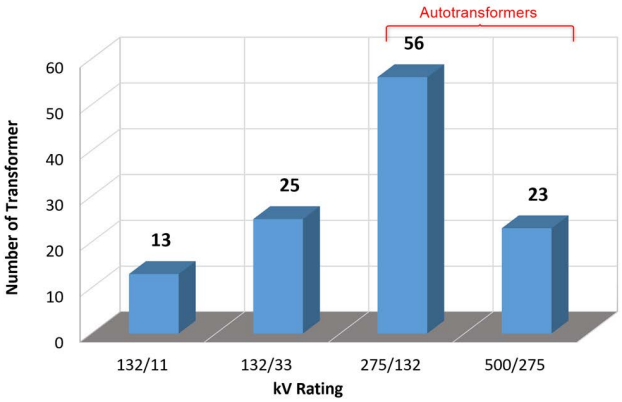

FIGURE 4. Number of 132 kV, 275 kV, and 500 kV transformers in the power network model.

American Electric Reliability Corporation (NERC), the vulnerability assessments of benchmark GMD events were set as a standard based on an occurrence frequency of 1 in 100 years [25]. Based on the assessments, a geoelectric field with a maximum strength of 12 V/km is applied to the system [26], [27], and if the generated GIC value is greater than 85 A/phase, the thermal analysis should be conducted. The benchmark GMD event is a uniform geoelectric field, which is assumed within a geographic region and calculated based on Equation (1).

$$E = V_{benchmark} \times \alpha \times \beta \,(\mathrm{V/km}) \tag{1}$$

where $V_{benchmark}$ represents the geoelectric field benchmark related to the 1 in 100 years GMD events, α (alpha) is the scaling factor considered for the local geomagnetic latitude, and β (beta) is the scaling factor considered for the local earth conductivity structure. Malaysia has only one magnetometer station located in Langkawi Island which can cover only the northern part of Peninsular Malaysia and there is a lack of geomagnetic coverage in the southern part of the country. Also, there is no magnetotelluric (MT) data available for Malaysia and detailed information regarding the earth's conductivity structure at the country scale. This forced us to use uniform ground conductivity values based on the 1-D earth conductivity data provided by the United States Geological Survey (USGS) [28] for β scaling factor. Different earth conductivity models were considered in this study such as shield, coastal, and mountain earth layered models. The NERC standard recommends the use of a particular USGS conductivity data as a substitute for unavailable specific regional conductivity data [29]. The α was set to 0.1 since the geomagnetic latitude of Malaysia is less than 7° according to the local geomagnetic latitude data [30]. These factors were multiplied by the benchmark geoelectric field based on Equation (1). The calculated electric fields with respect to these factors are presented in Table 1. These geoelectric fields consider more practical for low-latitude countries like Malaysia since they were calculated based on the local geomagnetic latitude and

TABLE 1. Calculated local electric fields with respect to 12 V/km benchmark geoelectric field and different scaling factors.

Scaling Factor (α)	Scaling Factor (β)	Calculated Electric Field (V/km)
0.1	Shield (1)	1.2
0.1	Coastal (0.81)	0.97
0.1	Mountain (0.56)	0.67

earth conductivity structure. Similar geoelectric field values have been used for GIC studies in other low-latitude countries such as South Korea [31], Spain [32], New Zealand [33], and Mexico [34].

The calculated geoelectric fields were uniformly applied throughout the Malaysian power network model, including the 132 kV network in different field directions of 0–180° via clockwise and intervals of 20° starting from the North as the effect of field angles on GIC could be investigated other than from the North or East direction. Additionally, it was unnecessary to calculate the GIC via other electric field directions, specifically 180–360°, as the GIC values would remain the same as the field points from the 0–180° direction except with different polarities. All substations in the uniform geoelectric electric field model experience the same field and induced voltages in the transmission lines depending on the assumed field direction [35]. Practically, the geoelectric fields are affected by the subsurface geology and ionospheric conditions and are not uniform in all locations. However, evaluating the power network using a uniform electric field would indicate substations that would experience large GIC and are considered critical exclusively due to the topology and orientation of the power network [36], [37]. In the PSS/E software, the induced DC voltages in the transmission lines are calculated according to Equation (2).

$$V_{ij} = \oint \vec{E} \circ \vec{dl} \tag{2}$$

Since the applied geoelectric fields in this work were assumed to be uniform over the power network model, thus, Equation (2) was simplified to Equation (3) by considering the geographic locations of the substations (endpoints of transmission lines) regardless of the routing twists and turns. Note that the true path of the power lines can lead to a more accurate GIC estimation. However, for this work, the line path data are unavailable.

$$V_{ij} = \vec{E} \circ \vec{L} = E_x L_x + E_y L_y \tag{3}$$

$$E_x = \mathrm{E} \cos\theta \tag{4}$$

$$E_y = \mathrm{E} \sin\theta \tag{5}$$

where $\vec{E}$ is the geoelectric field (V/km) along the transmission line, $\vec{L}$ is the length of the transmission line (km), E is the geoelectric field strength (V/km), E_x is the northward electric field (V/km), E_y is the eastward electric field (V/km), L_x is the northward line distance (km), L_y is the eastward line distance (km), and θ is the geoelectric field angle in degrees. There are several methods to calculate GIC in power grids. The most common methods are Lehtinen and Pirjola [38] and the nodal admittance matrix (NAM) methods [14], [39], [40]. The produced GIC across the network in the PSS/E software is calculated based on the NAM method. This method treats the network model as a DC equivalent circuit considering DC resistance parameters of system components since the GIC has a very low-frequency range. The NAM method calculates first the nodal voltages and the currents in the earthed conductor in a subsequent step based on Ohm's and Kirchoff's laws. The constructed DC equivalent circuit works for power grids with multiple voltage levels. The NAM method is mathematically equivalent to the LP method [41]. The DC model conversion of the multi-level voltages system including different transformer types, transmission lines and induced electric fields along the line are illustrated in Figs. 5 and 6.

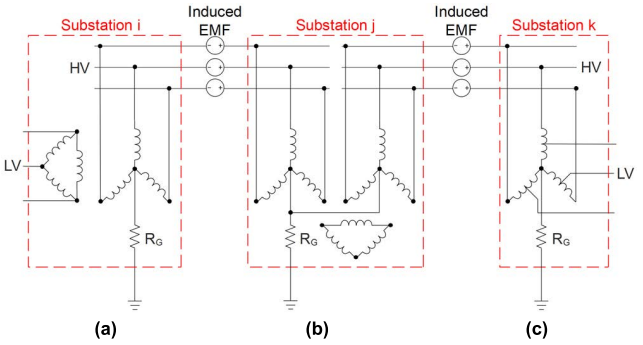

FIGURE 5. AC circuit of the multi-level voltage system including different transformer types (a) two winding, (b) three winding, and (c) auto with the induced electric field.

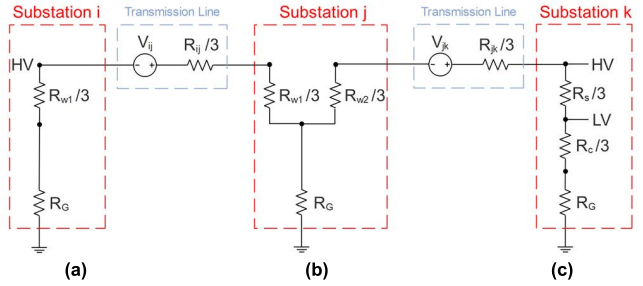

FIGURE 6. A single line DC equivalent circuit of the multi-level voltage system including different transformer types (a) two winding, (b) three winding, and (c) auto with the induced electric field.

Fig. 6 displays the DC equivalent model of the multi-level voltage system, where R_{w1} and R_{w2} are the HV and low voltage (LV) sides star winding resistances of the standard transformer, respectively. R_s and R_c are the series and common winding resistances of the autotransformer, respectively, and R_G is GR of the substations. R_{ij} and R_{jk} are the transmission lines resistances, and V_{ij} and V_{jk} are the induced voltage sources along the lines between the nodes. This DC model is then simplified more and presented in Fig. 7.

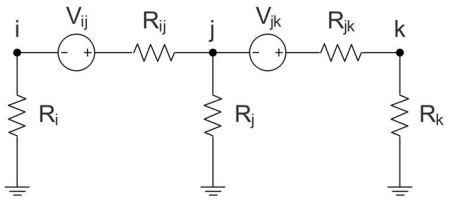

FIGURE 7. Three-bus DC equivalent circuit of power network with the induced electric field.

where R_i, R_j and R_k are the total resistances of substations, which include the winding resistance of the transformers and GR of the substations, R_{ij} and R_{jk} represent the resistances of connected transmission lines between the substations, and V_{ij} and V_{jk} represent the electric fields induced along the transmission lines. A single-phase equivalent circuit of all components is used to simplify a power network considering that the resistances of each phase in the circuit are assumed to be equal. Then using Norton's theorem, all circuit resistances are converted to the admittances and the induced electric field sources connected to the transmission lines are converted to the equivalent current sources and connected in parallel with the line admittances, as presented in Fig. 8.

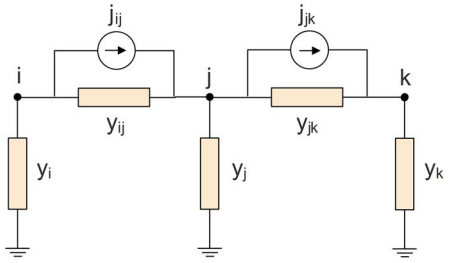

FIGURE 8. Three-bus DC equivalent circuit of power network based on Norton's theorem.

where y_i, y_j and y_k are the admittances of substations, y_{ij} and y_{jk} represent the admittances of transmission lines, and j_{ij} and j_{jk} represent the equivalent current sources along the lines. The parameters of y_{ij} and j_{ij} are defined in the following equations.

$$y_{ij} = \frac{1}{R_{ij}} \tag{6}$$

$$y_{ij} = -y_{ji} \tag{7}$$

$$Y_{ii} = y_i + \sum_{\substack{i \\ j=1}}^{n} y_{ij} \tag{8}$$

The summation of the equivalent currents at each node in Fig. 8 is defined as:

$$j_{ij} = \frac{V_{ij}}{R_{ij}} \tag{9}$$

$$J_i = j_{ji} \tag{10}$$

$$J_j = j_{ji} + j_{jk} \tag{11}$$

$$J_k = j_{kj} \tag{12}$$

The sum of flowing currents through line i, j is:

$$i_{ij} = j_{ij} + (v_i - v_j) y_{ij} \tag{13}$$

The matrix of Norton's currents is equal to

$$[J] = [Y][V] \tag{14}$$

where $[J]$ is the current source column matrix with elements [41], [42], $[Y]$ is the network admittance matrix and $[V]$ is the matrix of nodal voltage, so that from Equation (14), the nodal voltage is defined as:

$$[V] = [Y]^{-1}[J] \tag{15}$$

The flowing GIC through a neutral grounded transformer(s) in the network's node is represented as:

$$[\boldsymbol{I_{GIC}}] = [\boldsymbol{y_0}][\boldsymbol{Y}]^{-1}[\boldsymbol{J}] \tag{16}$$

where $[y_0]$ is the nodal admittance matrix. The reactive power losses of transformers at the normal exciting current without GIC can be calculated using Equation (17) [43].

$$Q = 3U_1 \cdot I_1 \tag{17}$$

where U_1 and I_1 are the voltage and fundamental harmonic values of the magnetization current in each phase, respectively. The reactive power losses of the transformers under the GIC condition are calculated from the following equation.

$$Q_{GIC} = k \cdot I_{eff} + Q \tag{18}$$

where k is the reactive power/ampere scaling factor, which is dependent on the core type of transformer [35], [44] and I_{eff} is the effective value of the GIC flowing in the transformer windings, which is dependent on the transformer type. The effective GIC calculations for the different transformers are presented in Equations (19–26). The calculation of effective GIC for the two winding transformers is presented in Equation 19.

$$I_{eff} = \left| \frac{NI_1 + I_2}{N} \right| \tag{19}$$

$$N = \frac{N_1}{N_2} = \frac{V_1}{V_2} \tag{20}$$

where I_1, I_2, V_1, V_2, N_1, and N_2 are the currents, voltages and numbers of turns of the transformer's windings at the primary and secondary sides, respectively. For two winding autotransformers, the effective GIC is calculated as follows:

$$I_{eff} = \left| \frac{(N-1)I_s + I_c}{N} \right| \tag{21}$$

$$N = \frac{N_s + N_c}{N_c} = \frac{V_1}{V_2} \tag{22}$$

where I_s, I_c, N_s, and N_c are the currents and number of turns of the series and common windings of the autotransformer, respectively. The calculation of effective GIC for the three winding transformers is presented in Equation (23).

$$I_{eff} = \left| \frac{N_{13} I_{eff\,12} + I_3}{N_{13}} \right| \tag{23}$$

$$N_{13} = \frac{N_1}{N_3} = \frac{V_1}{V_3} \tag{24}$$

$$I_{eff\,12} = \left| \frac{N_{12} I_1 + I_2}{N_{12}} \right| \tag{25}$$

$$N_{12} = \frac{N_1}{N_2} = \frac{V_1}{V_2} \tag{26}$$

where I_3, V_3, and N_3 are the current, voltage, and number of turns of the transformer's third winding, respectively. Since the k-factor was set at 1 for all the available transformers in the power model in this study, the reactive power consumptions of the transformers under the GIC condition are almost the same as effective GICs, as illustrated in Equation (18). In the calculation, the value of reactive power of transformers without GIC condition (Q) is assumed to be zero. Because the GIC calculations based on the DC model consider only the DC resistances of the nodes which have physical connections to the ground and all power sources, delta windings of transformers and loads are ignored since they do not provide the GIC flow paths. While in a real scenario, the power system is under the operating condition when it is exposed to GMD events so that the reactive power under GIC condition (Q_{GIC}) will be added to the actual reactive power of the transformer (Q).

Power utilities are particularly concerned over unusual reactive power demand due to voltage stability issues and reactive power reserve scheduling [16]. Significant variations in the active and reactive power balance could cause fluctuations in the system and reduce the efficiency of the transformer [45]. Additionally, a sudden increase of the reactive power in the system could overload and trip capacitive components, such as static var compensators (SVCs) in the system, contributing to grid instability [46] and leading to permanent transformer damage or blackouts [19]. Ultimately, this would result in a cumulative loss in the economic revenue for the power sector and the nation [47], [48].

III. RESULTS AND DISCUSSION

In this section, the calculation of GIC in the Malaysian power network was carried out through three scenarios, including the system under normal operating condition, and benchmark GMD events with and without consideration of 132 kV lower voltage systems. The results of these simulation scenarios are presented and discussed in detail in the following subsections.

A. SYSTEM UNDER NORMAL OPERATING CONDITION

After the data of the Malaysian power network were gathered and the 138 bus system was completed in PSS/E, the entire network model was evaluated under normal operating condition. The simulation result was obtained without GIC to investigate and ensure the performance and efficiency of the system as well as to establish the initial conditions for other studies since the power network was firstly built based on an actual AC system, including loads and power sources. The power flow solution of the system was developed using the PSS/E software. Note that the PSS/E is considered one of the most powerful simulation tools for performing load flow and other power network analyses.

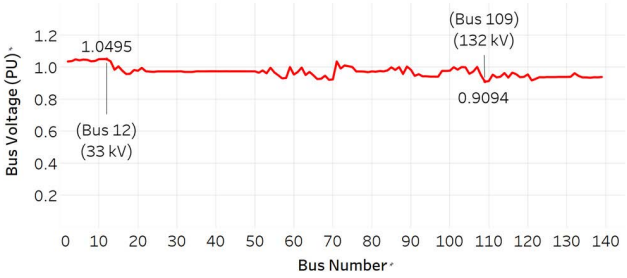

FIGURE 9. Results of the system bus voltages.

Fig. 9 shows that the magnitudes of bus voltages are within acceptable limits of the voltage variation requirements according to grid and distribution codes for Peninsular Malaysia at normal operating condition, as presented in Table 2 [21], [22], [23].

TABLE 2. Steady-state voltage variation.

Nominal Voltage	% Variation of Nominal Voltage
6.6 kV, 11 kV, 22 kV, 33 kV	± 5%
132 kV and 275 kV	± 10%
500 kV	± 5%

According to Table 2, all bus voltages were within the permissible limits between 0.90 pu and 1.10 pu. The reason of the voltage fluctuation between the buses is that the 54 substations network model in this study was designed for the GIC analysis and did not include all available system components, such as capacitive or inductive var support, transformer tap settings, and other power generators that work to maintain the system voltage limits [49]. The pu value is used to easily represent and compare different voltage levels from one side of the transformer to the other.

B. ESTIMATED GIC IN THE POWER NETWORK

In this case, the GIC values at the different parts of the system were calculated by applying benchmark geoelectric fields uniformly to the entire power network presented in Fig. 2 with different storm angles of 0–180° in clockwise direction with intervals of 20° starting from the North. We first applied 1.2 V/km geoelectric field magnitude which was calculated based on 1 in 100 years of GMD events occurrence frequency considering the α and β scaling factors of the local geomagnetic latitude and shield earth conductivity structure respectively, as presented in Table 1. The GIC calculations were carried out using a GIC analysis tool in PSS/E software which was based on the NAM method. The resulting GIC flows and total reactive power losses were computed across the system individually for each angle.

Fig. 10 shows the absolute values of the GIC results at different substations across the Malaysian power network due to

the 1.2 V/km applied geoelectric field at 0° (northward) and 100° (roughly eastward) field angles. In the figure, the GIC results are presented in a blue circle when the entire network model that includes 500 kV, 275 kV, and 132 kV systems are considered and in a red circle when only 500 kV and 275 kV systems are considered, in other words when 132 kV low voltage systems were removed from the analysis. Note that only the graphs for these two angles were presented to highlight the significance of the results since they contributed the highest GICs. Fig. 10(a) shows that substations located at the edge of the power network are the most affected by northward geoelectric fields and experience GIC intensities. The highest GICs were obtained at substations 4 and 22 with values of 36.47 A and 37.78 A due to 1.2 V/km with 132 kV system consideration, as depicted in a blue circle.

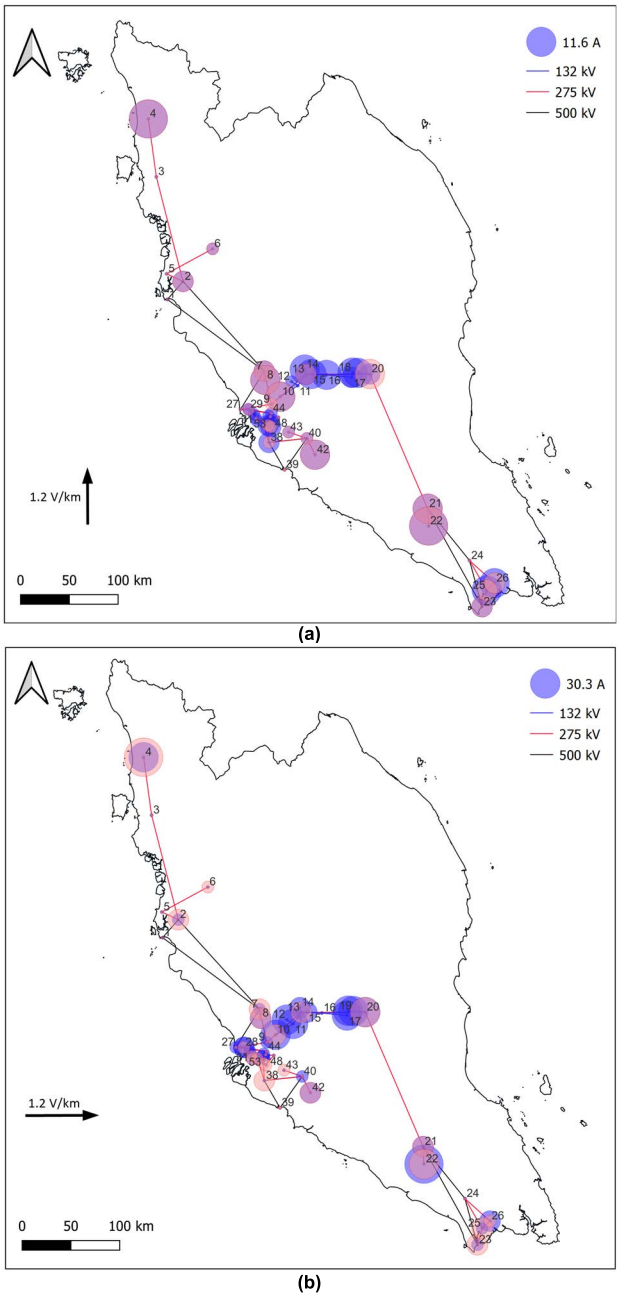

FIGURE 10. The absolute GICs at the earthing point of each substation due to the 1.2 V/km geoelectric field at (a) 0° and (b) 100° field directions when the model was exclusively for the 500 kV and 275 kV networks (red circles) and when we added the 132 kV network (blue circles).

After the applied geoelectric field angle was changed to a 100° eastward direction, the GIC values across the system also changed. The most severe GICs were observed in the substations in the middle of the Malaysian power network, especially substations (17, 19, 21 and 22), as noticed in Fig. 10(b), compared to the impact at 0° angle. The maximum GIC was obtained at substation 22 with a value of 44.58 A due to a 1.2 V/km applied geoelectric field, including a 132 kV system, as presented as a blue circle. Therefore, substation 22 was considered one of the most critical locations in the system affected by GMD. The largest GIC will be produced if the substations or transmission lines between them are parallel to the geoelectric field. In contrast, transmission lines that are perpendicular to the geoelectric fields result in a zero GIC [36]. Additionally, the increased GIC values in the middle of the system were contributed by the longer transmission lines connected to these substations, as illustrated in Fig. 11 since the longer lines allowed greater induced DC voltages (Equation 2). The substation GIC is the total GIC observed at the neutral common ground path of the transformers. This GIC is divided based on the number of ground-connected star winding transformers that defers from one substation to another.

Certain substations might possess multiple neutral grounds for different transformer banks or rated voltages. However, in this study, a single common neutral ground was used at each station. The GIC amplitudes obtained from the 1.2 V/km benchmark geoelectric field were smaller than the maximum allowable GIC flow of 75 A/phase in the transformer, as highlighted in the NERC guideline. This allowable threshold current was related to the operational stability of the power system, the heating limit of the transformer winding and the iron core, and the local overheating limitation of the structural parts in the transformer. Additionally, this simulation case showed that the susceptibility of the Malaysian power network to GICs closely resembled that of the South Korean power system since the maximum GICs obtained for both systems due to the 1.2 V/km applied benchmark geoelectric field were almost similar [31].

Compared to other worldwide power networks, the Malaysian network was less susceptible to GMD since smaller GICs were induced in the system, as presented in Table 3. From the table, it can be seen that the Norwegian [50], Spanish [51], New Zealand [33], Irish [36], Mexican [34] and the IEEE benchmark test system in US power networks produced larger GICs due to the 1 V/km uniform applied geoelectric field. This was due to the network span of those countries that covered a much larger area than the Malaysian power network since a larger transmission network produced larger induced voltage and GIC [52]. Moreover, the different outcome was influenced by the varying

TABLE 3. Comparison of the maximum GIC result between the Malaysian power grid and other power grids worldwide due to uniform geoelectric fields.

Country	Applied geoelectric field (V/km)	Angle (degree)	GIC (A)
Malaysia	1.2	100°	44.58
Korea [31]	1.2	0°	51.13
Norway [50]	1	0°	151.10
Spain [51]	1	90°	141
New Zealand [33]	1	45°	≥ 185
Ireland [36]	1	90°	113
Mexico [34]	1	90°	≥ 180
IEEE Test System in the US [37]	1	90°	354.52

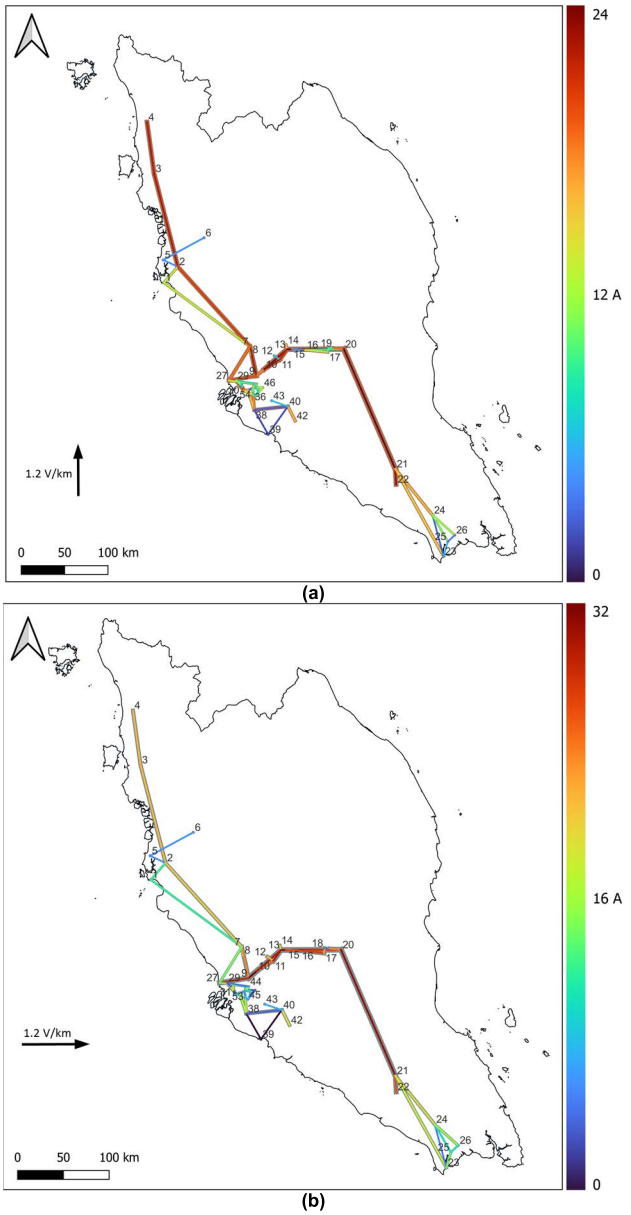

FIGURE 11. The absolute GICs (A/phase) along the transmission lines, including 132 kV systems and (considering the total currents when the lines are multiple) due to the 1.2 V/km geoelectric field at (a) 0° and (b) 100° field directions. The colour bar on the right indicates the colour coding for the GICs.

network parameters (resistances and topology) compared to the power networks in Peninsular Malaysia [4].

In order to assess the sensitivity of the calculated GICs in the Malaysian system, we have also looked at how removing a 132 kV lower voltage system in the power grid would affect GICs. Fig 10 shows that the calculated GICs were slightly increased when a lower voltage system was removed from the network model, especially at substations 10–21 and 27–50, since the 132 kV network in this study was linked between these substations (Fig. 2). The only exception to this was the substations 21 and 22, which experienced a slight decrease in the calculated GIC. In other words, the addition of the 132 kV network decreased the calculated GICs in some substations due to the inclusion of the additional GIC flow path in the 132 kV transformers in the model and currents directed into the lower voltage substations [53] (Fig. 11).

In Fig. 12, we compared the GICs results across substations due to other geoelectric field magnitudes on the entire network which were calculated based on other earth conductivity models such as shield, coastal, and mountains, as presented in Table 1.

The figure shows that the actual GICs tend to remain either positive or negative at a particular site throughout the modelled storms [54]. Since the magnitudes of applied geoelectric fields due to the coastal and mountain earth conductivity models are less than the applied field of the shield model, the GIC intensities of the substations are decreased. The results obtained in this work can be used to plan the installation of GIC mitigation systems at the most critical substations in the middle of the Malaysian power network, as highlighted in Fig. 12(b). Furthermore, the results justify the need to assess the grid response in case of GMD events. Since the GICs flow through the winding of the neutral grounded transformers available in the power network causes half-cycle saturation of transformer cores and leads to increase reactive power losses in the system, we calculated the reactive power consumptions of transformers in the system under GMD events to look for its dangerousness. Fig. 13 shows the results of reactive power losses summations of different transformers' types available in the entire network for a benchmark 1.2 V/km electric field in the 0–180° orientations.

From the figure, the maximum sums of reactive power losses in the 132/33 kV two winding and 132/11 kV three winding transformers in the Malaysian system were obtained due to a 1.2 V/km geoelectric field at 80° field angle with values of 28.2 and 39.1 Mvar, as presented in orange and blue colours, respectively. These values strongly depend on the

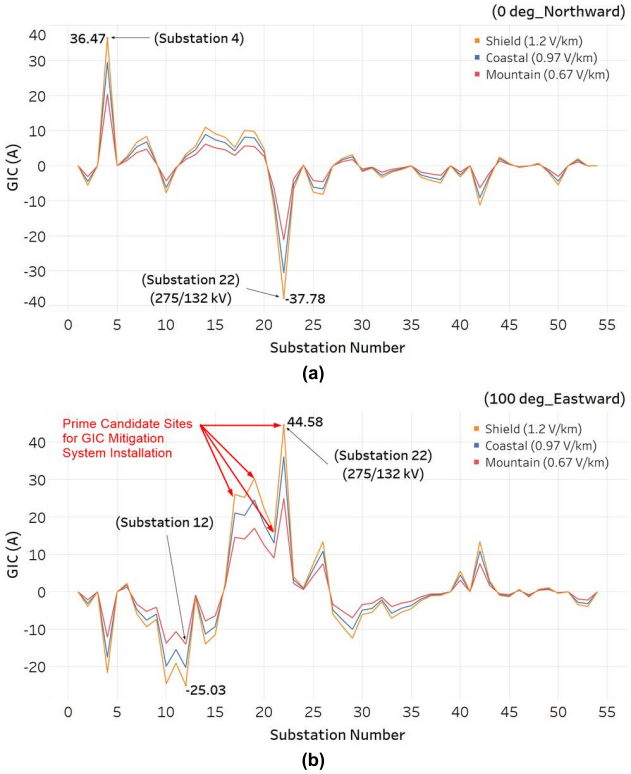

FIGURE 12. The GICs at the earthing point of each substation due to the 1.2 V/km geoelectric field at (a) 0° and (b) 100° field directions considering different earth conductivity models. Positive GIC (flowing into the bus) and negative GIC (flowing into the ground).

FIGURE 13. The cumulative sum of reactive power losses in the different transformer types in the Malaysian power due to the 1.2 V/km benchmark electric field directed at 0–180° angles.

number of available transformers types in the power network and their location concerning the applied geoelectric field orientation. This indicates that an 80° angle experienced the most impactful GIC effect on such types of transformers in the system. Since both 500/275 kV and 275/132 kV are three winding autotransformers, their results were combined together. The maximum sum of reactive power losses for three winding autotransformers in the system was observed at 140° storm angle with a value of 87.3 Mvar. This could be expected because the 500 kV and 275 kV systems in Peninsular Malaysia have different locations and more transformers in the model (a total of 79 transformers) than the 132 kV system.

In terms of the total sum of the reactive power losses in all transformers in the Malaysian power network model in this simulation case, the figure shows that an electric field pointing at 100° induced maximum reactive power losses in the whole network with a total cumulative value of 144.3 Mvar. This roughly eastward angle was the most impactful geoelectric field angle with respect to the overall power network model since it covers most parts of the system and contributes the highest induced currents and reactive power consumption with respect to all transformer types in the model rather than a single transformer type. Therefore, it was considered the worst-case scenario field angle in the overall system. Noteworthy, in Fig. 13 can be seen that the sums of reactive power losses for 132/33 kV two winding transformers, 132/11 kV three winding transformers, and three winding autotransformers in the network at 100° field angle are 27.2, 38.5, and 78.6 Mvar, respectively which total is 144.3 Mvar. Meaning that the sum of reactive power losses realized at 100° storm direction may not be the maximum sum for any specific transformer, as shown in the figure, but it is the worst among the group of transformers in the system. The vulnerability of different types of transformers to GMD events depends on their design and they are not equally prone to GIC consequences [51]. Since the induced current is a phenomenon that affects all transformers simultaneously in a large geographical area, the increase of reactive power demand was associated with a summation of all transformers [43].

The impact of the 132 kV addition was also examined with respect to the increased reactive power demands in the system due to the 1.2 V/km at different field directions. Fig. 14 compares the increased total GICs and reactive power demands for the 500 kV and 275 kV systems with and without the 132 kV system. The figure illustrates a slight increase in the overall effective GICs and reactive power demands in most field angles when the lower voltage was removed from the model. The major sum of reactive power losses in the system without a lower voltage system was obtained at a 140° field angle with a value of 89.78 Mvar. Note that the comparison results were obtained for the three winding autotransformers since they were the only available type in the 500 kV and 275 kV systems (Fig. 4).

This analysis highlighted the importance and impact of the inclusion of lower voltage systems on the computed GICs in the HV power network. Lower voltage systems are less critical in the GIC calculations since they have larger resistance parameters than higher voltage levels. However, recent findings have shown that lower voltage networks could significantly impact the calculated GICs [32], [55] and neglecting them may cause a slight overestimation in the GIC

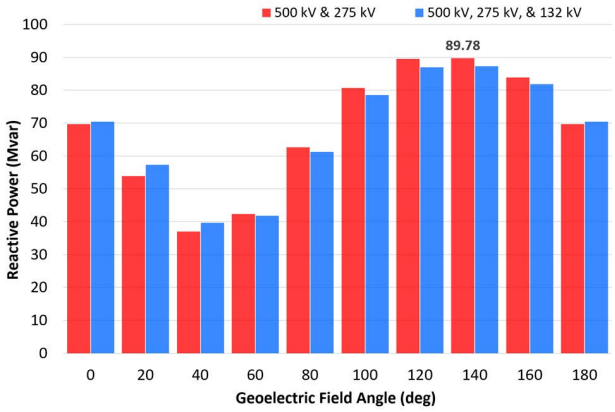

FIGURE 14. The cumulative sum of reactive power losses in all transformers in the Malaysian power network due to the 1.2 V/km at 0–180° angles from North with and without 132 kV power network, as depicted in blue and red, respectively.

results [34]. This is highly dependent on the configuration of an individual network [56].

IV. CONCLUSION

This study presented and discussed numerical simulations of GIC analysis in a power system network in Peninsular Malaysia using PSS/E software. The network included 500 kV, 275 kV, and 132 kV transmission systems. The GICs have been computed and observed in the power network model due to uniform benchmark geoelectric fields in a different direction in the 0–180° field angles with and without 132 kV lower voltage systems. The geoelectric field magnitudes were computed based on 1 in 100 years of GMD events occurrence with consideration of the local geomagnetic latitude of Malaysia and different earth conductivity models. The maximum modelled geoelectric field magnitude was 1.2 V/km. The results showed that eastward geoelectric fields produced the maximum GICs and reactive power losses for most of the transformers available in the system. Also, the results demonstrated that substations 4, 17, 19, 21, and 22 where are located in the middle and edge of the network were the most vulnerable to GMD events and experienced the highest GIC values. The maximum value of GIC was observed at substation 22 for most geoelectric field angles 0–180°, especially 100° eastward field orientation induced GIC with a value of 44.58 A when a 1.2 V/km geoelectric field was applied to the system. This indicates that substation 22 is the most vulnerable location in the Malaysian power grid to the GMD events and 100° eastward field orientation is considered the most impactful field angle with respect to the Malaysian grid.

In comparison to other global power networks, however, the results showed that the Malaysian power network was less susceptible to GIC effects with respect to the same field value. In addition, when the 132 kV lower voltage system was disconnected from the network model, the GICs in most substations and reactive power losses were slightly increased, especially from the nodes directly linked to such system. In contrast, other nodes that do not have direct connections were less affected. The variation rate was also dependent on the storm direction. Although the model has limitations because of assumptions regarding the spatial uniformity of applied geoelectric field and conductivity models, it can be used to understand the GMD impacts on the power grid and the flow of GICs in the system more generally. In short, the simulation results have established several new findings that have not been reported in the past regarding the GIC effects analysis on the Malaysian power network model. Also, the results have presented clear guidelines which help system operators to expect and forecast large GIC and take actions to avoid problems in case of space weather. Based on the overall analysis results that were obtained in this work. The local power utility is recommended to install GIC mitigation systems in the substations located in the middle of the power network, especially substation 22 since it experienced the highest GIC value to protect the system from any future GMD events. Furthermore, it is necessary to provide additional magnetic stations in the Malaysian territory and pursue a GIC analysis based on more accurate and realistic calculated geoelectric fields.

REFERENCES

[1] S. P. Blake, P. T. Gallagher, J. McCauley, A. G. Jones, C. Hogg, J. Campanyà, C. D. Beggan, A. W. P. Thomson, G. S. Kelly, and D. Bell, "Geomagnetically induced currents in the Irish power network during geomagnetic storms," *Space Weather*, vol. 14, no. 12, pp. 1136–1154, Dec. 2016.

[2] S. K. Vijapurapu, "Contingency analysis of power systems in presence of geomagnetically induced currents," M.S. thesis, Elect. Comput. Eng., Univ. Kentucky, Lexington, KY, USA, 2013.

[3] J. Ramírez-Niño, C. Haro-Hernández, J. H. Rodriguez-Rodriguez, and R. Mijarez, "Core saturation effects of geomagnetic induced currents in power transformers," *J. Appl. Res. Technol.*, vol. 14, no. 2, pp. 87–92, Apr. 2016.

[4] R. Pirjola and D. Boteler, "Geomagnetically induced currents in European high-voltage power systems," presented at the Can. Conf. Elect. Comput. Eng., 2006.

[5] D. Bejmert, K. Boehme, M. Kereit, and W. Rebizant, "HV transformer protection and stabilization under geomagnetically induced currents," *Energies*, vol. 13, no. 18, p. 4693, Sep. 2020.

[6] W. H. Barlow, "VI. On the spontaneous electrical currents observed in the wires of the electric telegraph," *Phil. Trans. Roy. Soc. London*, vol. 139, pp. 61–72, Dec. 1849.

[7] A. Karsberg, G. Swedenborg, and K. Wyke, "The influences of earth magnetic currents on telecommunication lines," *Tele English Ed., Televerket (Swedish Telecom)*, vol. 1, pp. 1–21, Jan. 1959.

[8] W. H. Campbell, "Observation of electric currents in the Alaska oil pipeline resulting from auroral electrojet current sources," *Geophys. J. Int.*, vol. 61, no. 2, pp. 437–449, May 1980.

[9] A. Pulkkinen, "Geomagnetic induction during highly disturbed space weather conditions: Studies of ground effects," Academic Dissertation, Dept. Phys. Sci., Finnish Meteorological Inst., Helsinki, Finland, 2003.

[10] J. G. Kappernman and V. D. Albertson, "Bracing for the geomagnetic storms," *IEEE Spectr.*, vol. 27, no. 3, pp. 27–33, Mar. 1990.

[11] T. S. Molinski, "Why utilities respect geomagnetically induced currents," *J. Atmos. Solar-Terr. Phys.*, vol. 64, no. 16, pp. 1765–1778, Nov. 2002.

[12] J. Koen and C. Gaunt, *Geomagnetically Induced Currents at Mid-Latitudes*. Maastricht, The Netherlands: International Union of Radio Science (URSI) General Assembly, 2002.

[13] B. Dong, Z. Wang, R. Pirjola, C. Liu, and L. Liu, "An approach to model Earth conductivity structures with lateral changes for calculating induced currents and geoelectric fields during geomagnetic disturbances," *Math. Problems Eng.*, vol. 2015, pp. 1–10, Jan. 2015.

[14] R. Caraballo, "Geomagnetically induced currents in uruguay: Sensitivity to modelling parameters," *Adv. Space Res.*, vol. 58, no. 10, pp. 2067–2075, Nov. 2016.

[15] A. A. Hussein and M. H. Ali, "Suppression of geomagnetic induced current using controlled ground resistance of transformer," *Electr. Power Syst. Res.*, vol. 140, pp. 9–19, Nov. 2016.

[16] N. Chiesa, A. Lotfi, H. K. Høidalen, B. Mork, Ø. Rui, and T. Ohnstad, "Five-leg transformer model for GIC studies," in *Proc. Int. Conf. Power Syst. Transients (IPST)*, Vancouver, BC, Canada, 2013, pp. 1–6.

[17] Z. M. K. Abda, N. F. A. Aziz, M. Z. A. A. Kadir, and Z. A. Rhazali, "A review of geomagnetically induced current effects on electrical power system: Principles and theory," *IEEE Access*, vol. 8, pp. 200237–200258, 2020.

[18] Z. M. Khurshid, N. F. A. Aziz, Z. A. Rhazali, and M. Z. A. A. Kadir, "Impact of geomagnetically induced currents on high voltage transformers in Malaysian power network and its mitigation," *IEEE Access*, vol. 9, pp. 167204–167217, 2021.

[19] T. Hutchins, "Geomagnetically induced currents and their effect on power systems," M.S. thesis, Elect. Comput. Eng., Univ. Illinois Urbana-Champaign, Champaign, IL, USA, 2012.

[20] C. Liu, Y. Li, and R. Pirjola, "Observations and modeling of GIC in the Chinese large-scale high-voltage power networks," *J. Space Weather Space Climate*, vol. 4, p. A03, Jan. 2014.

[21] T. N. Berhad, *Transmission System Reliability Standards*. Malaysia: Tenaga Nasional Berhad, 2006.

[22] (2020). *Grid Code for Peninsular Malaysia, T. N. Berhad, Malaysia*. [Online]. Available: https://www.gso.org.my/GridCode/GridCode.aspx

[23] F. T. Sabahm and T. N. Labuan. (2017). *Distribution Code for Peninsular Malaysia*. [Online]. Available: https://www.st.gov.my/en/contents/publications/guidelines_electricity/2017/Distribution%20Code%20For%20Peninsular%20Malaysia%20Sabah%20%20F.T.%20Labuan%20Amendments%202017_V5.pdf#:~:text=The%20amendments%20of%20the%20Distribution,other%20distributed%20generation%20into%20the

[24] T. J. Overbye, T. R. Hutchins, K. Shetye, J. Weber, and S. Dahman, "Integration of geomagnetic disturbance modeling into the power flow: A methodology for large-scale system studies," in *Proc. North Amer. Power Symp. (NAPS)*, Sep. 2012, pp. 1–7.

[25] A. Pulkkinen, E. Bernabeu, J. Eichner, C. Beggan, and A. W. P. Thomson, "Generation of 100-year geomagnetically induced current scenarios," *Space Weather*, vol. 10, no. 4, Apr. 2012, Art. no. 04003.

[26] L. Winter, "Geomagnetically induced currents from extreme space weather events," in *Geomagnetically Induced Currents From Sun to Power Grid*. Hoboken, NJ, USA: Wiley, 2019, ch. 11, pp. 195–203.

[27] M. Kazerooni and T. J. Overbye, "Mitigating power system response to GICs in known networks," in *Geomagnetically Induced Currents From Sun to Power Grid*. Hoboken, NJ, USA: Wiley, 2019, ch. 13, pp. 219–232.

[28] (2017). *New Reliability Standard NERC TPL-007-1, N. A. E. R. Corporation, US*. [Online]. Available: https://ccaps.umn.edu/documents/CPE-Conferences/MIPSYCON-PowerPoints/2017/TutITransmissionSystemPerformanceforGeomagneticDisturbanceEvents.pdf

[29] S. N. Backhaus and M. K. Rivera, *Review of the GMD Benchmark Event in TPL-007-1*. Los Alamos, NM, USA: Los Alamos National Lab. (LANL), 2015.

[30] NERC. (2016). *Benchmark Geomagnetic Disturbance Event Description*. [Online]. Available: https://www.nerc.com/pa/Stand/TPL0071RD/Benchmark_clean_May12_complete.pdf

[31] B.-S. Joo, J.-W. Woo, J.-H. Lee, I. Jeong, J. Ha, S.-H. Lee, and S. Kim, "Assessment of the impact of geomagnetic disturbances on Korean electric power systems," *Energies*, vol. 11, no. 7, p. 1920, Jul. 2018.

[32] J. M. Torta, S. Marsal, and M. Quintana, "Assessing the hazard from geomagnetically induced currents to the entire high-voltage power network in Spain," *Earth, Planets Space*, vol. 66, no. 1, p. 87, Dec. 2014.

[33] K. Mukhtar, M. Ingham, C. J. Rodger, D. H. Mac Manus, T. Divett, W. Heise, E. Bertrand, M. Dalzell, and T. Petersen, "Calculation of GIC in the north island of new Zealand using MT data and thin-sheet modeling," *Space Weather*, vol. 18, no. 11, Nov. 2020, Art. no. e2020SW002580.

[34] R. Caraballo, J. A. González-Esparza, M. Sergeeva, and C. R. Pacheco, "First GIC estimates for the Mexican power grid," *Space Weather*, vol. 18, no. 2, Feb. 2020, Art. no. e2019SW002260.

[35] S. Dahman. *Modeling GMD in PowerWorld Simulator*. PowerWorld Corporation. Accessed: 2019. [Online]. Available: https://www.powerworld.com/files/G02_GMD_In_Simulator.pdf

[36] S. Blake, "Modelling and monitoring geomagnetically induced currents in Ireland," Trinity College Dublin., Dublin, Ireland, School Phys., Tech. Rep., 2017.

[37] R. Horton, D. Boteler, T. J. Overbye, R. Pirjola, and R. C. Dugan, "A test case for the calculation of geomagnetically induced currents," *IEEE Trans. Power Del.*, vol. 27, no. 4, pp. 2368–2373, Oct. 2012.

[38] M. Lehtinen and R. Pirjola, "Currents produced in earthed conductor networks by geomagnetically-induced electric fields," *Annales Geophysicae*, vol. 3, no. 4, pp. 479–484, 1985.

[39] D. Boteler, "Methodology for simulation of geomagnetically induced currents in power systems," *J. Space Weather Space Climate*, vol. 4, p. A21, Jan. 2014.

[40] R. Pirjola, "Properties of matrices included in the calculation of geomagnetically induced currents (GICs) in power systems and introduction of a test model for GIC computation algorithms," *Earth, Planets Space*, vol. 61, no. 2, pp. 263–272, Feb. 2009.

[41] D. H. Boteler and R. J. Pirjola, "Comparison of methods for modelling geomagnetically induced currents," *Annales Geophys.*, vol. 32, no. 9, pp. 1177–1187, Sep. 2014.

[42] D. H. Boteler and R. J. Pirjola, "Modeling geomagnetically induced currents," *Space Weather*, vol. 15, no. 1, pp. 258–276, Jan. 2017.

[43] S. A. Mousavi and D. Bonmann, "Analysis of asymmetric magnetization current and reactive power demand of power transformers due to GIC," *Proc. Eng.*, vol. 202, pp. 264–272, Jan. 2017.

[44] X. Dong, Y. Liu, and J. G. Kappenman, "Comparative analysis of exciting current harmonics and reactive power consumption from GIC saturated transformers," in *Proc. IEEE Power Eng. Soc. Winter Meeting. Conf.*, Jan. 2001, pp. 318–322.

[45] J. Kappenman, "Geomagnetic storms and their impacts on the U.S. power grid," Metatech Corporation, Goleta, CA, USA, Tech. Rep., Meta-R-319, 2010.

[46] R. Girgis and K. Vedante, "Effects of GIC on power transformers and power systems," in *Proc. PES (T&D)*, May 2012, pp. 1–8.

[47] A. Rajan, T. Sanjay, and Venkatesh, "Impact of geomagnetically induced current on high voltage direct current converters and transformers," *J. Adv. Res. Dyn. Control Syst.*, vol. 10, pp. 791–799, Apr. 2018.

[48] D. M. Oliveira and C. M. Ngwira, "Geomagnetically induced currents: Principles," *Brazilian J. Phys.*, vol. 47, no. 5, pp. 552–560, Oct. 2017.

[49] (2018). *Power Systems Analysis*, I. Standards, New York, NY, USA. [Online]. Available: https://mentor.ieee.org/3000-stds/dcn/19/stds-19-0002-00-PUBS-3002-2.pdf

[50] M. Myllys, A. Viljanen, Ø. A. Rui, and T. M. Ohnstad, "Geomagnetically induced currents in Norway: The northernmost high-voltage power grid in the world," *J. Space Weather Space Climate*, vol. 4, p. A10, Jan. 2014.

[51] J. M. Torta, S. Marsal, J. Ledo, P. Queralt, V. Canillas-Pérez, P. Piña-Varas, J. J. Curto, A. Marcuello, and A. Martí, "New detailed modeling of GICs in the Spanish power transmission grid," *Space Weather*, vol. 19, no. 9, Sep. 2021, Art. no. e2021SW002805.

[52] R. A. Marshall, A. Kelly, T. Van Der Walt, A. Honecker, C. Ong, D. Mikkelsen, A. Spierings, G. Ivanovich, and A. Yoshikawa, "Modeling geomagnetic induced currents in Australian power networks," *Space Weather*, vol. 15, no. 7, pp. 895–916, Jul. 2017.

[53] J. Kappenman, *Low-Frequency Protection Concepts for the Electric Power Grid: Geomagnetically Induced Current (GIC) and E3 HEMP Mitigation*. Goleta, CA, USA, 2010.

[54] G. S. Kelly, A. Viljanen, C. D. Beggan, and A. W. P. Thomson, "understanding GIC in the U.K. and French high-voltage transmission systems during severe magnetic storms," *Space Weather*, vol. 15, no. 1, pp. 99–114, Jan. 2017.

[55] S.-X. Guo, L.-G. Liu, R. J. Pirjola, K.-R. Wang, and B. Dong, "Impact of the EHV power system on geomagnetically induced currents in the UHV power system," *IEEE Trans. Power Del.*, vol. 30, no. 5, pp. 2163–2170, Oct. 2015.

[56] C. D. F. Barroso, *GIC Distribution*. Stockholm, Sweden: Lund Univ., 2014.

ZMNAKO MOHAMMED KHURSHID received the Technical Diploma degree in electrical engineering from the Kalar Technical Institute, Iraq, in 2007, the B.Eng. degree in electrical and electronic engineering from the Asia Pacific University of Technology & Innovation (APU), Malaysia, in 2015, the M.Sc. degree from Universiti Putra Malaysia, Malaysia (UPM), in 2018, and the Ph.D. degree in electrical engineering from Universiti Tenaga Nasional (UNITEN), Malaysia, in 2022. His current research interests include hybrid systems, particularly that contain renewable energy, such as PV systems and wind turbines, lightning and lightning transient effects, and geomagnetically induced current (GIC) on electrical power systems.

NUR FADILAH AB AZIZ (Member, IEEE) received the Master of Engineering degree (Hons.) in electrical engineering from the University of Southampton, U.K., in 2006, and the Ph.D. degree from Universiti Teknologi Mara, Shah Alam, in 2014. She is currently a Senior Lecturer with the Department of Electrical and Electronics Engineering, Universiti Tenaga Nasional (UNITEN), Malaysia. She is also a Graduate Member of the Board of Engineers Malaysia (BEM). Her research interests include power system analysis, renewable energy, fault identification and location, distribution automation, statistical pattern recognition, artificial intelligent (AI), and machine learning application in power systems.

ZETI AKMA RHAZALI received the bachelor's degree in electrical, electronics and system engineering from Universiti Kebangsaan Malaysia, in 1996, and the Ph.D. degree in electrical engineering from Universiti Malaysia Pahang, in 2014. She has worked as the Head of the Department of Electronic and Communication Engineering, College of Engineering, Universiti Tenaga Nasional (UNITEN), from 2018 to 2019. She was a Senior Engineer (Research and Development), from 1996 to 2001, with vast experiences in telecommunication technologies and advancements related to mobile radio, space, and satellite communications. She is currently the Head of the Department of Engineering Foundation and Diploma Studies, College of Engineering, UNITEN. She is also a Professional Engineer (P.Eng.) registered with the Board of Engineers (BEM) Malaysia and a member of The Institution of Engineers (IEM), Malaysia. Her research interests include antenna synthesis and analyses, microwave and milimeter wave engineering and the ionospheric communication studies.

MOHD ZAINAL ABIDIN AB KADIR (Senior Member, IEEE) received the B.Eng. degree in electrical and electronic engineering from Universiti Putra Malaysia and the Ph.D. degree in high voltage engineering from the University of Manchester, U.K. Currently, he is a Strategic Hire Professor at the Institute of Power Engineering (IPE), Universiti Tenaga Nasional (UNITEN), and a Professor at the Faculty of Engineering, Universiti Putra Malaysia. He is also the Founding Director of the Centre for Electromagnetic and Lightning Protection Research (CELP), Universiti Putra Malaysia. He is also an IEEE Power & Energy Society (PES) Distinguished Lecturer in the field of lightning and high voltage engineering. To date, he has authored or coauthored over 350 journals and conference papers. His research interests include high voltage engineering, lightning protection, electromagnetic compatibility, power system transients, and renewable energy. He is also a Professional Engineer (P.Eng.), a Chartered Engineer (C.Eng.), and a Professional Technologist (P.Tech.). He is also the Chairperson of the National Mirror Committee of IEC TC 81 (Lightning Protection) and a Local Convener of MNC-CIGRE C4 on System Technical Performance. He is also an Advisory Board Member of the National Lightning Safety Institute (NLSI), USA, and a Research Advisor of the African Centre for Lightning and Electromagnetic (ACLE).